

Electrostatic waves near the lower hybrid frequency*

R. L. Stenzel and W. Gekelman

Department of Physics, University of California, Los Angeles, California 90024

(Received 10 October 1974; revised manuscript received 2 December 1974)

The propagation of slow electrostatic waves across a magnetic field \vec{B}_0 ($k_{\parallel}^2 / k_{\perp}^2 \lesssim m_e / m_i$) near the lower hybrid frequency ($\omega \gtrsim \omega_{LH}$) has been investigated experimentally in a large uniform magnetoplasma. The dispersion is in good agreement with the fluid description; warm-plasma effects appear near $k_{\perp} r_{ci} \simeq 2\pi$. Propagation of wave packets reveals the dispersive and backward wave nature of the modes ($v_g > 0$, $v_{ph} < 0$, $v_g \ll |v_{ph}|$), the different directions of phase and group velocity ($\omega/\vec{k} \sim \perp \partial\omega/\partial\vec{k} \sim \parallel \vec{B}_0$) and the cone structure of the antenna radiation pattern.

The lower hybrid resonance has attracted a great deal of interest in connection with rf heating of plasmas. It is predicted¹⁻³ that in a weakly nonuniform plasma an incident electromagnetic wave ($\vec{k} \sim \parallel \nabla n \perp \vec{B}_0$, where \vec{k} is the wave vector for the incident wave, n is the plasma density, and \vec{B}_0 is the confining field), can propagate to the lower hybrid resonance layer [$\omega_{LH}(r) = \omega_0$], where it has changed its character to a slow electrostatic wave. This wave is absorbed by collisional damping ($\nu/\omega > 5 \times 10^{-5}$) or, in collisionless plasmas, converted to a slow warm-plasma mode which is damped by wave-particle interactions. An experiment on the linear mode conversion has been reported in the literature⁴ but it was performed in such a small nonuniform plasma column ($n/\nabla n \approx \lambda_{\perp}$) that a detailed study of the wave propagation was not possible.

It is the purpose of this paper to report first direct dispersion measurements of the electrostatic waves at and above the lower hybrid frequency. In contrast to all other experiments^{4,5} we excite the waves with a fine wire grid *inside* the *uniform* region of a large magnetized plasma. This approach first ensures wave penetration into the plasma, which is difficult to achieve with external exciter plates in a finite-length system since the energy flow is almost parallel to \vec{B}_0 . Second, the plasma uniformity prevents wave refraction which complicates dispersion measurements unless the gradients are weak ($n/\nabla n \gg \lambda$). Lower hybrid waves with wavelengths as short as the ion Larmor radius ($r_{ci} \approx 1.5$ mm) are observed. The measured dispersion relation is in good agreement with the predictions from cold-plasma theory except for finite-temperature effects very close to the resonance ($k_{\perp} r_{ci} \lesssim 2\pi$).⁶ Group-velocity measurements with phase-coherent wave bursts verify the backward-wave properties and the different directions of phase velocity and energy flow within a conical radiation pattern.

The experiment is performed in a large (15 cm

diam, 150 cm length), quiescent ($\delta n/n \lesssim 1\%$), weakly collisional ($\nu/\omega \approx 10^{-2}$), magnetized ($B_0 \approx 1000$ G), steady-state discharge plasma (helium, $n_e \approx 10^{10}$ cm⁻³, $kT_e \approx 2.5$ eV, $kT_i \approx 0.25$ eV). The plasma device is described in detail elsewhere.⁷ The plasma diagnostics consist of small Langmuir probes (orbital regime) and an X-band interferometer. Propagation of electron Bernstein waves ($\perp \vec{B}_0$) and ion acoustic waves ($\parallel \vec{B}_0$) yield further independent information about ω_{pe} , T_e , T_i , and collision rates.

Lower hybrid waves are launched from a 95-cm-long excited grid of smallest possible surface area (an array of 14 electrically connected, plane-parallel, spring-loaded 0.1-mm-diam W wires, 35 mm total height) immersed into the uniform center region (approx 8 cm diam) parallel to \vec{B}_0 (see Fig. 1). The waves are detected with three identical

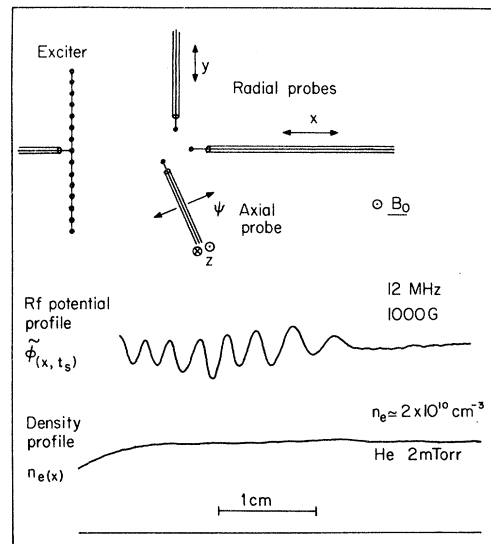


FIG. 1. Axial view of exciter grid and receiver probes (top), typical sampled wave potential vs radial position (middle), and radial density profile (bottom).

T probes (3 cm length, 0.1 mm diam, 1 mm o.d. coaxial feed), movable in axial direction, radial direction parallel and perpendicular to the exciter grid surface normal, respectively.

Phase-coherent wave bursts ($10 < f < 30$ MHz, $V_0 \lesssim 1$ V) with approximately Gaussian envelopes are applied to the floating exciter grid. The received signals are processed with wide-band amplifiers and a sampling oscilloscope. Most measurements are performed after the end of the applied wave burst so as to avoid the large capacitively coupled signal.

The measured dispersion relation ω vs k_\perp at two different densities is shown in Fig. 2. The data were taken at small exciter amplitudes and the linearity was verified. The error bar in ω indicates the frequency spread of the wave packet. The perpendicular wave number is determined from two orthogonal wavelength measurements across the field [$k_\perp = 2\pi(\lambda_x^{-2} + \lambda_y^{-2})^{1/2}$], since the wave was found to propagate at an angle of about 30° with respect to the exciter-grid surface normal.⁸ Direct measurements of the parallel wavelength with the axial probe were not possible since the probe cannot be moved accurately enough along a field line (to within $\Delta r \ll \lambda_\perp \sim 3$ mm over axial

distances $\Delta z > L_{\text{exc}} \approx 1000$ mm). For comparison with theory,¹ which in the cold-plasma approximation predicts the dispersion relation

$$\omega = \omega_{\text{LH}} \left(1 + \frac{k_\parallel^2}{k_\perp^2 + k_\perp^2 \frac{m_i}{m_e}} \right)^{1/2}, \quad (1)$$

where $\omega_{\text{LH}} \approx \omega_{\text{pi}} (1 + \omega_{\text{pe}}^2 / \omega_{\text{ce}}^2)^{-1/2}$ is the lower hybrid frequency, we have matched *one* experimental datum point (ω^*, k_\perp^*) to the theoretical curve (solid line in Fig. 2) and obtained $\lambda_\parallel \approx 32$ cm.⁹ Subsequently, all other data points fall on the predicted dispersion curve to within experimental error. Even at a different density the agreement is good. Note that in each case the lower hybrid frequency is determined independently from density and field measurements. Conversely, the dispersion measurement may become a useful density diagnostic tool.

Although cold-plasma theory predicts $k_\perp \rightarrow \infty$ as $\omega \rightarrow \omega_{\text{LH}}$ we have not been able to observe wavelengths shorter than the ion Larmor radius ($r_{ci} \approx 1.5$ mm). This cannot be the result of inadequate probe resolution since the same probes can resolve even shorter wavelength electron-cyclotron harmonic waves ($\lambda_\perp < 1$ mm, $f \approx 2000$ MHz) but it indicates the finite-temperature modification of the wave dispersion relation.⁶

The dispersion relation predicts opposite signs for phase and group velocities perpendicular to \vec{B}_0 . This backward-wave property is clearly observed in the propagation of phase coherent-wave bursts as shown in Fig. 3. While the wave packet moves in time away from the exciter [Fig. 3(a)] the phase fronts approach it [Fig. 3(b), expanded time scale].

The waves are damped before reaching the plasma boundaries, thus no reflections are seen. Damping results from electron-neutral collisions and low-frequency density fluctuations which destroy the phase coherence of the waves [$k_\perp = k_\perp(\omega_p^2)$]. The regime of short wavelengths cannot be explored when the noise level exceeds a few percent as is typical in rf-produced plasmas.

The wave-packet measurements directly verify the predicted slow perpendicular group velocity ($v_{g\perp} < v_{ph\perp} \ll v_e$). Along the field, however, Eq. (1) predicts a much larger group velocity, $v_{g\parallel} = (k_\perp/k_\parallel)v_{g\perp}$. The resulting wave propagation from the exciter structure is schematically shown in Fig. 4 (top). While the wave energy (\vec{v}_g) leaves the exciter at a small angle $\pm\theta$ ($\theta^2 < m_e/m_i$) the phase fronts approach the antenna with $\vec{v}_{ph} \sim \pm \vec{v}_g$. The propagation is symmetric in z but for purpose of a clear display only one direction is sketched. This predicted propagation pattern is confirmed by the probe data in Fig. 4 (bottom) which display the

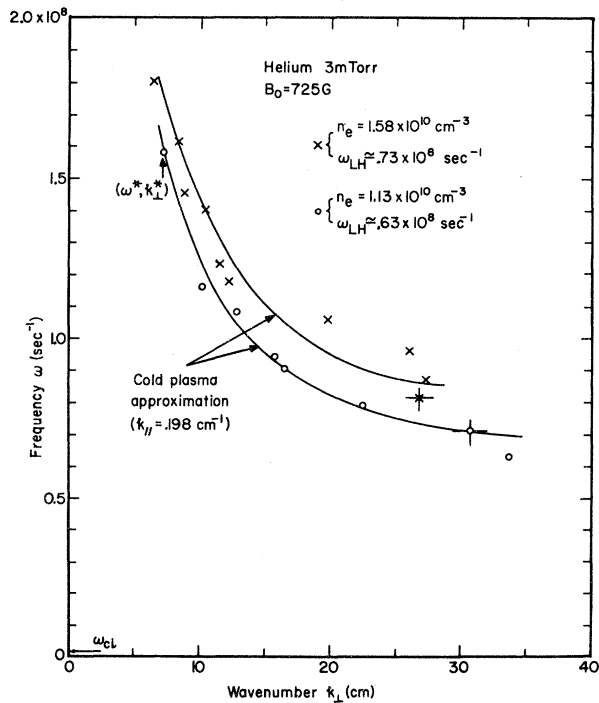


FIG. 2. Dispersion of lower hybrid waves ($\omega > \omega_{\text{LH}}$). Solid curves are cold-plasma approximation, crosses and circles are data points at two different densities. The parallel wavelength is determined by data matching at a single point (ω^*, k_\perp^*).

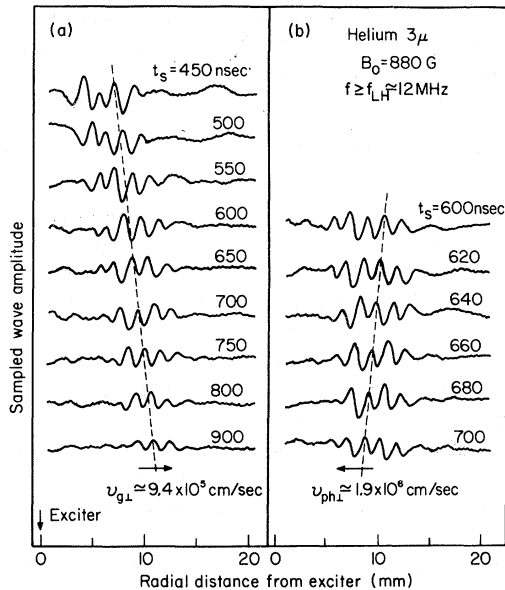


FIG. 3. Propagation of a phase coherent-wave burst demonstrating the backward-wave behavior of lower hybrid waves. Fig. 3(a) shows the wave packet moving away from the exciter while Fig. 3(b) displays for a shorter time interval the phase fronts approaching the exciter.

wave amplitude versus radial position in the middle of the exciter sampled at different times after the end of an applied long tone burst. First we note that no waves are visible at any time beyond a certain radial position corresponding to a cone at angle θ .¹⁰ At early times the entire cone region is filled with waves. With increasing time one observes first the disappearance of waves close to the exciter which involves short distances of propagation and last on the cone edge where the wave packets have traveled along $\frac{1}{2}L_{exc}$. The axial-group delay time yields $v_{g\parallel} \gg v_{g\perp}$ which is independently confirmed from axial-probe measurements of the arrival of wave packets beyond the ends of

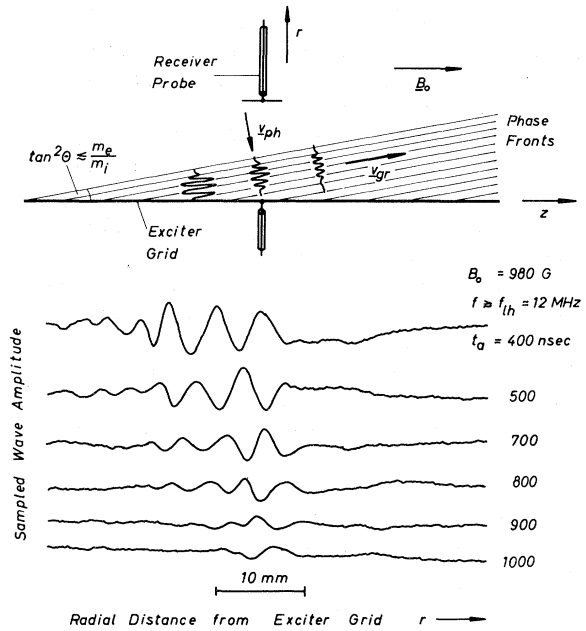


FIG. 4. Top: schematic picture of lower hybrid wave propagation from the exciter grid for a single mode k_z in a uniform plasma. Bottom: sampled wave amplitude vs radial position in the middle of the exciter at different times after the end of an applied long tone burst.

the exciter ($v_{g\parallel} \sim 10^8$ cm/sec).

On the cone edge the long temporal decay of the signal is governed by the axial-group delay time ($L_{exc}/2v_{g\parallel}$) which as expected is found to be independent of the applied-burst length. We have reduced the applied-burst length to a single pulse ($\Delta t \sim 50$ nsec) and observed ringing responses up to 1 μ sec at a frequency corresponding closely to ω_{LH} and scaling properly with varying density.

The authors gratefully acknowledge valuable discussions with A. Y. Wong, G. Morales, P. Vandénplas, and R. W. Gould. The expert technical support by Z. Lucky is greatly appreciated.

*Work supported by the Atomic Energy Commission.

¹T. H. Stix, *The Theory of Plasma Waves* (McGraw-Hill, New York, 1962), Chaps. 2 and 3; Phys. Rev. Lett. **15**, 878 (1965).

²A. D. Piliya and V. I. Fedorov, Zh. Eksp. Teor. Fiz. **57**, 1198 (1969) [Sov. Phys.—JETP **30**, 653 (1970)].

³P. Bellan and M. Porkolab, Phys. Rev. Lett. **34**, 124 (1975).

⁴W. M. Hooke and S. Bernabei, Phys. Rev. Lett. **28**, 407 (1972).

⁵P. L. Colestock and W. D. Getty, Bull. Am. Phys. Soc. **18**, 1290 (1973); P. Bellan and M. Porkolab, Bull. Am. Phys. Soc. **19**, 955 (1974).

⁶A. M. Messiaen and P. E. Vandénplas, Plasma Phys. **15**, 505 (1973); S. Puri and M. Tutter, Max-Planck Institut für Plasmaphysik, Garching bei München, report IV/71, 1974 (unpublished).

⁷W. Gekelman and R. L. Stenzel, Rev. Sci. Instrum. (to be published).

⁸The asymmetry remains unchanged with reversal of \vec{B}_0 hence does not appear to result from an $\vec{E} \times \vec{B}_0$ drift.

⁹The excitation of a finite parallel wavelength with a linear exciter appears to contradict the theoretical predictions of Ref. 3. However, in our experiment there is a small axial periodicity in the B field at the exciter location caused by the finite solenoid coil spacing d

($d = \lambda_{\parallel} = 32$ cm). Thus the excited phase fronts are periodically inclined with respect to \vec{B}_0 . Since the lower hybrid waves propagate typically at angles $\frac{1}{2}\pi \pm 1\%$ with respect to \vec{B}_0 even a very small periodic field curvature is sufficient to define k_{\parallel} .

¹⁰Wave propagation along conical surfaces are observed

with small exciter structures: R. K. Fisher and R. W. Gould, Phys. Fluids 14, 857 (1971); R. J. Briggs and R. R. Parker, Phys. Rev. Lett. 29, 852 (1972). In our experiment the wave-number spread is small and the energy flows within the cone volume rather than along its surface.